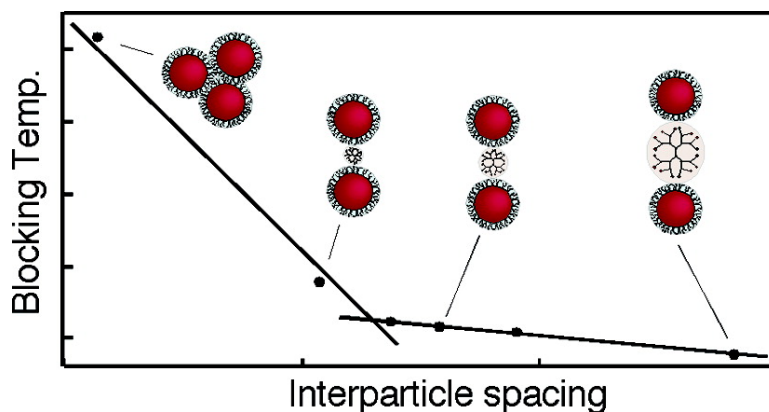


Direct Control of the Magnetic Interaction between Iron Oxide Nanoparticles through Dendrimer-Mediated Self-Assembly

Benjamin L. Frankamp, Andrew K. Boal, Mark T. Tuominen, and Vincent M. Rotello

J. Am. Chem. Soc., **2005**, 127 (27), 9731-9735 • DOI: 10.1021/ja051351m • Publication Date (Web): 18 June 2005

Downloaded from <http://pubs.acs.org> on March 25, 2009



More About This Article

Additional resources and features associated with this article are available within the HTML version:

- Supporting Information
- Links to the 21 articles that cite this article, as of the time of this article download
- Access to high resolution figures
- Links to articles and content related to this article
- Copyright permission to reproduce figures and/or text from this article

[View the Full Text HTML](#)

Direct Control of the Magnetic Interaction between Iron Oxide Nanoparticles through Dendrimer-Mediated Self-Assembly

Benjamin L. Frankamp,[†] Andrew K. Boal,[†] Mark T. Tuominen,[‡] and Vincent M. Rotello^{*,†}

Contribution from the Departments of Chemistry and Physics, University of Massachusetts, Amherst, Massachusetts 01003

Received March 3, 2005; E-mail: rotello@chem.umass.edu

Abstract: Cationic superparamagnetic iron oxide nanoparticles were assembled using a series of anionic polyamidoamine dendrimers. The resulting assemblies featured systematically increasing average interparticle spacing over a 2.4 nm range with increasing dendrimer generation. This increase in spacing modulated the collective magnetic behavior by effective lowering of the dipolar coupling between particles. The results obtained in these studies deviate from the predicted dependence of collective behavior on interparticle spacing, suggesting that a dense assembly of magnetically “free” particles can exist with a surprisingly small space between particles.

Magnetic materials are key components in modern technology, with applications ranging from data storage¹ to magnetic resonance imaging contrast agents.² The next generation of these materials will rely on a fundamental understanding of nanometer-sized domains as features become increasingly smaller. Magnetic nanoparticles represent a critical link between current technology and future applications due to their unique size-dependent properties³ which include superparamagnetism,⁴ a state where the net magnetic moment of single domain particle is zero based on ambient thermal activation.⁵ Particle–particle interactions can play a significant role in modulating the magnetic behavior of a collection of particles, falling into two main categories: exchange coupling⁶ and magnetostatic interactions.⁷ The challenge is to first understand the fundamental interactions between nanometer-sized domains and then develop methods in terms of both particle fabrication and self-assembly that will allow us to tailor these interactions as needed.

Dipolar magnetostatic interactions of magnetic nanoparticles are currently studied by statistically diluting particles in an inert medium.⁸ This method has established several correlations

between interparticle spacing and collective behavior, yet several unresolved conflicts remain between experimental data and theoretical prediction. In addition, this method cannot provide data at very high particle concentrations due to agglomeration.⁹ A new strategy based on the direct manipulation of the interparticle spacing, and thus interaction, of each particle would be advantageous from a fundamental point of view and could potentially lead to new materials with tailored properties.

One viable method to create such materials entails judicious use of molecular self-assembly to create tailored magnetic nanoparticle structures. Molecular self-assembly is an attractive assembly tool because it can be used to specifically associate components in solution using noncovalent interactions, in turn facilitating “bottom up” fabrication of nanoscale materials.¹⁰ Current research in our group has focused on the development of methods to control the self-assembly of nanoparticles using a variety of molecular interactions.¹¹ In one such study, polyamidoamine (PAMAM) dendrimers were used to assemble particles using electrostatic interactions, resulting in an increase in average interparticle spacing based on dendrimer generation.^{11c} The demonstrated ability to directly control interparticle spacing in a nanoparticle-based system prompted us to investigate the fundamental interaction of magnetic nanoparticles using a similar strategy. This approach allows us to circumvent the issue of agglomeration at high particle concentrations while enabling

[†] Department of Chemistry.

[‡] Department of Physics.

- (1) (a) Farhoud, M.; Hwang, M.; Smith, H. I.; Bae, J. M.; Youcef-Toumi, K.; Ross, C. A. *IEEE Trans. Magn.* **1998**, *34*, 1087–1089. (b) Kryder, M. H. *MRS Bull.* **1996**, *21*, 17–22.
- (2) Pankhurst, Q. A.; Connolly, J.; Jones, S. K.; Dobson, J. *J. Phys. D: Appl. Phys.* **2003**, *36*, R167–R181.
- (3) (a) Battle, X.; Labarta, A. *J. Phys. D: Appl. Phys.* **2002**, *35*, R15–R42. (b) Hu, J. T.; Li, L. S.; Yang, W. D.; Manna, L.; Wang, L. W.; Alivisatos, A. P. *Science* **2001**, *292*, 2060–2063.
- (4) Néel, L. *C. R. Acad. Sci.* **1949**, *228*, 664.
- (5) For uniaxial, spherical nanoparticles the activation energy follows as $E_A = KV \sin^2 \theta$, where K is the anisotropy constant, V is the volume of the particle, and θ is the angle between the magnetization and the easy magnetic axis. See: (a) Stoner, E. C.; Wohlfarth, E. P. *Philos. Trans. R. Soc. London A* **1948**, *240*, 599. (b) Pfeiffer, H. *Phys. Stat. Sol. (a)* **1990**, *122*, 377–389.
- (6) Herzer, G. *IEEE Trans. Magn.* **1989**, *25*, 3327–3329. Giri, A. K.; Chowdary, K. M.; Humfeld, K. D.; Majetich, S. A. *IEEE Trans. Magn.* **2000**, *36*, 3026–3028.
- (7) (a) Dormann, J. L.; Fiorani, D.; Tronc, E. *Adv. Chem. Phys.* **1997**, *98*, 283–494. (b) Russier, V.; Petit, C.; Pileni, M. P. *Phys. Rev. B* **2000**, *62*, 3910–3916.

- (8) Vestal, C. R.; Song, Q.; Zhang, Z. *J. Phys. Chem. B* **2004**, *108*, 18222–18227.
- (9) (a) Webb, B. C.; Schultz, S.; Oseroff, S. B. *J. Appl. Phys.* **1988**, *63*, 2923–2925. (b) Leslie-Pelecky, D. L.; Rieke, R. D. *Chem. Mater.* **1996**, *8*, 1770–1783.
- (10) (a) Bowden, N. B.; Weck, M.; Choi, I. S.; Whitesides, G. M. *Acc. Chem. Res.* **2001**, *34*, 231–238. (b) Le, J. D.; Pinto, Y.; Seeman, N. C.; Musier-Forsyth, K.; Taton, T. A.; Kiehl, R. A. *Nano Lett.* **2004**, *4*, 2343–2347.
- (11) (a) Boal, A. K.; Ilhan, F.; DeRouchey, J. E.; Thurm-Albrecht, T.; Russell, T. P.; Rotello, V. M. *Nature* **2000**, *404*, 746–748. (b) Frankamp, B. L.; Uzun, O.; Ilhan, F.; Boal, A. K.; Rotello, V. M. *J. Am. Chem. Soc.* **2002**, *124*, 892–893. (c) Frankamp, B. L.; Boal, A. K.; Rotello, V. M. *J. Am. Chem. Soc.* **2002**, *124*, 15146–15147. (d) Srivastava, S.; Frankamp, B. L.; Rotello, V. M. *Chem Mater.* **2005**, *17*, 487–490.

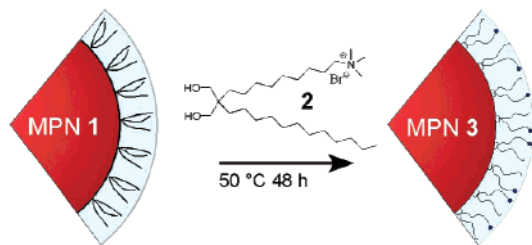


Figure 1. Surface exchange of diol **2** onto MPN **1** to provide functional magnetic nanoparticle MPN **3**.

us to determine interparticle interactions through choice of dendrimer.¹² Furthermore, it provides a means to find an optimal interparticle spacing to mitigate interparticle interactions while retaining maximum particle density.

Here we report the synthesis, functionalization, and characterization of the self-assembly of magnetic nanoparticles and a series of PAMAM dendrimers. In these assemblies, we observed a clear dependence of the average interparticle spacing on dendrimer generation using small-angle X-ray scattering (SAXS). Upon assembly with a series of PAMAM dendrimers, we were able to create a set of samples that featured systematically increasing spacing of ~ 2.4 nm between extremes. This structural manipulation resulted in a shift in the blocking temperature of greater than 50 K. Given this dramatic shift in the collective behavior upon directed self-assembly, we are able to make two key observations concerning the system. First, in contrast to theoretical predictions of uniform r^3 dependence between interparticle spacing on blocking temperature, our data suggest that there are two distinct regimes: an initial interdependence of approximately r^6 , followed by a dramatic leveling off at larger interparticle distances. Second, upon assembly with the largest dendrimer, we observe magnetic behavior identical to that of particles free of magnetic interactions, suggesting that the assembled particles were fully decoupled within the dense aggregate.

Results and Discussion

To create a magnetic nanoparticle suitable for molecular self-assembly, a suitable monolayer was fabricated and exchanged onto the magnetic core, synthesized following a method reported by Alivisatos and co-workers.¹³ Previously researchers from our laboratory reported a concise method to functionalize the surface of magnetic nanoparticles using a 1,3-diol moiety as an anchor to the particle surface.²³ MPN **1**, a 5.4 ± 1.2 nm alkylamine-capped precursor particle, was exchanged with diol ligand **2**, providing in MPN **3** as shown in Figure 1.

Two critical features of our assembly strategy are outlined in Figure 2a. First, the ratio and concentration of nanoparticle and dendrimer were carefully chosen to ensure that an excess of dendrimer is present during the initial stages of the assembly process, leading to complete coating of dendrimer on each particle. Once this initial complex is formed, dendrimer is embedded between adjacent particles, allowing us to dictate the interparticle spacing by changing the dendrimer generation.¹⁴ Furthermore, this method ensures that interparticle spacing is homogeneous throughout the sample. This is in contrast to

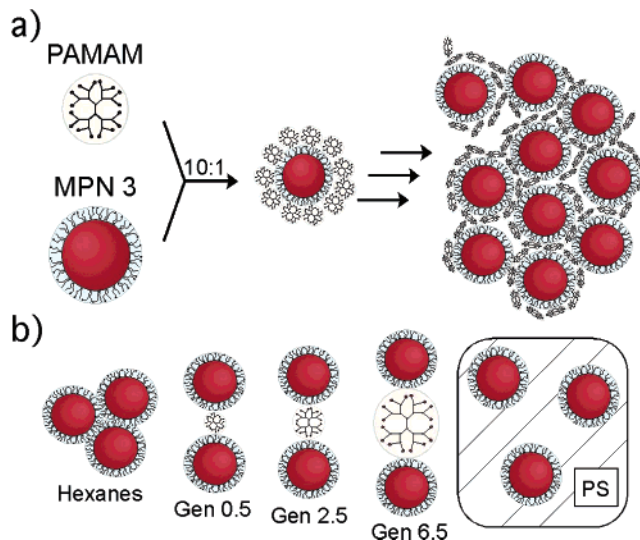


Figure 2. (a) Schematic depiction of dendrimer-mediated nanoparticle assembly. (b) Increase in average interparticle spacing upon assembly with PAMAM dendrimers, as well as hexane and polystyrene controls.

standard dilution research where a small population of agglomerated particles could bias the average interparticle spacing or, more importantly, influence the collective magnetic behavior. In addition we looked at two controls: particles precipitated in the absence of dendrimer (hexanes) and particles dispersed in a polystyrene (PS) matrix (Figure 2b). The precipitated particles represented a strongly coupled sample while particles dispersed in PS represented a fully decoupled sample.

SAXS was used to quantify the interparticle spacing of adjacent MPN **3** particles upon dendrimer-mediated self-assembly. As expected, there was an increase in spacing with increasing dendrimer generation (Figure 3).¹⁵ An overall increase of ~ 2.4 nm between particles in the absence of dendrimer and those assembled with the largest dendrimer generation 6.5 is consistent with previous results.¹¹

To determine the effect of interparticle spacing on the collective magnetic behavior of the resultant nanocomposites, we performed temperature- and field-dependent measurements using a superconducting quantum interference device (SQUID). As mentioned earlier, superparamagnetism is a state where the thermal energy in a system is greater than the barrier present in the particle holding the magnetization in a certain direction. Upon cooling, the thermal energy in the system decreases and the energy barrier increases, locking the magnetization along the direction of the easy axis, resulting in a net dipole.¹⁶ This blocking temperature is directly dependent on the volume of the magnetic nanoparticle. Since each sample in our system was prepared from the exact same batch of particles, eliminating core discrepancies, we were able to directly investigate the change in dipolar interactions versus interparticle spacing.

Zero-field-cooled (ZFC) and field-cooled (FC) measurements were collected in a single run with an applied field of 100 Oe.

(12) For alternate methods of forming close-packed, tunable magnetic composites, see: (a) Tartaj, P.; Serna, C. J. *Chem. Mater.* **2002**, *14*, 4396–4402. (b) Vestal, C. R.; Zhang, Z. J. *Nano Lett.* **2003**, *12*, 1739–1743.
(13) Rockenberger, J.; Scher, E. C.; Alivisatos, A. P. *J. Am. Chem. Soc.* **1999**, *121*, 11595–11596.

(14) See earlier dendrimer assembly work (ref 11c), where low ratios of dendrimer relative to nanoparticle gave rise to assemblies based on nanoparticle–nanoparticle interactions.

(15) The q value is related to distance by a simple inverse relationship: $q = 2\pi/d$.

(16) The thermal transition between paramagnetic behavior and ferromagnetic behavior is the blocking temperature and can be directly related to several factors shown in $T_B = KV/(\ln(\tau_{exp}/\tau_0))k_B$, where K is the anisotropy constant, $25k$ is a good approximation of standard laboratory measurement constants ($\ln(\tau_{exp}/\tau_0)$), V is the particle volume, and k_B is equal to the Boltzmann factor.

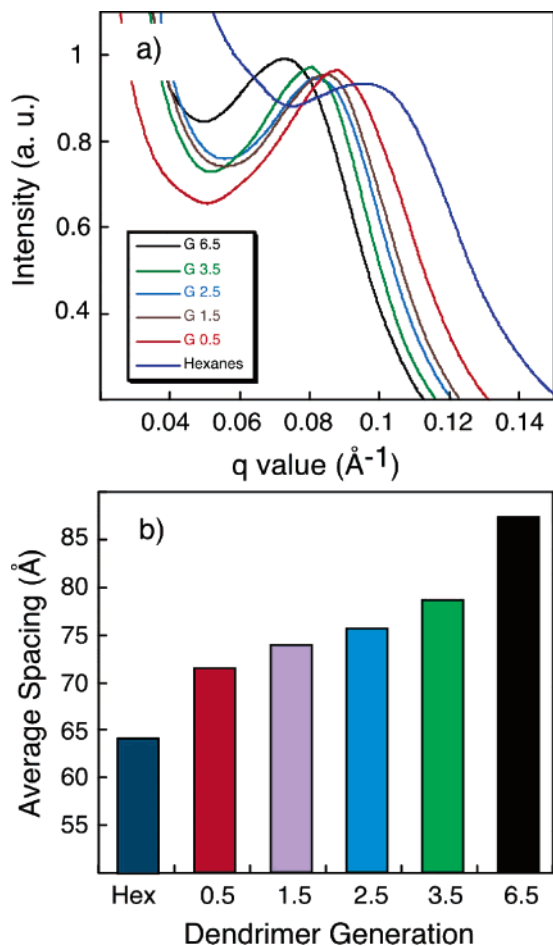


Figure 3. (a) SAXS plots shown after background subtraction and normalization. (b) The systematic increase in interparticle spacing as the PAMAM generation increased. (Average spacing: d (Å) = $2\pi/q$).

Particles that precipitated in the absence of dendrimer were separated only by their monolayers, providing the largest blocking temperature of 83 K. Upon assembly with increasing generation dendrimers the blocking temperature decreased, resulting in a value of 29 K with generation 6.5 (Figure 4). Field-dependent SQUID characterization at 1.8 K allowed us to obtain values of coercivity (H_C) and reduced remanence (M_R/M_S) on each sample (Figure 5 and Table 1). As expected, the hexanes control sample showed a lower M_R/M_S of 0.30 than the assembled samples, presumably due to increased magnetic coupling present in the more closely spaced sample.¹⁷ The H_C values also showed a subtle increase (25 Oe) between hexanes control and assembled samples (Table 1).¹⁸ Both the M_R/M_S and H_C are dependent on increasing interparticle interactions; however, this dependence is not as pronounced as that of the T_B data.¹⁹

Our results are consistent with the Dormann–Bessais–Fiorani²⁰ model that predicts that interparticle interactions will increase the activation energy E_A by a factor B_i (eq 1). An

$$E_A = KV \sin^2 \theta + B_i \quad (1)$$

increase in the activation energy would explain the observed

(17) Held, G. A.; Doyle, G. H.; Sun, S.; Murray, C. B. *Phys. Rev. B* **2001**, *64*, 012408(4).

(18) See Supporting Information for full hysteresis measurements from each sample.

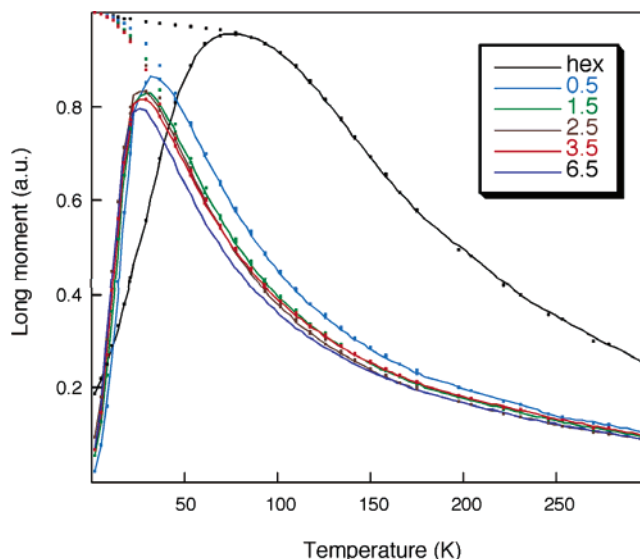


Figure 4. FC and ZFC magnetization plots for each sample, showing the steady decrease in T_B as the particles are spaced farther apart from one another.

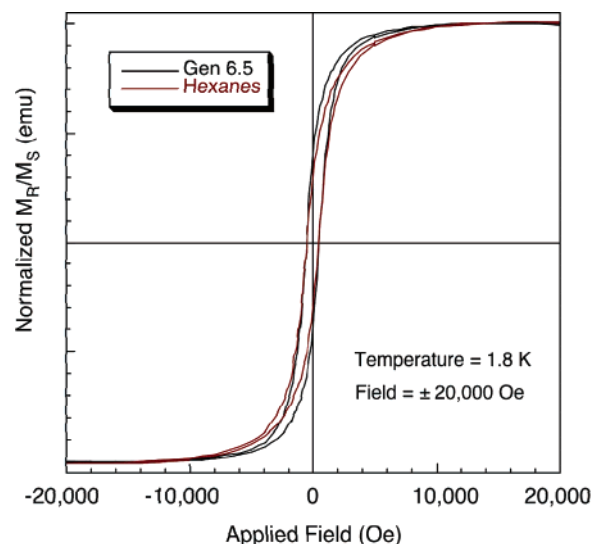


Figure 5. Representative hysteresis measurements of MPN 3 assembled with G6.5 (black) and hexanes control (red) with an applied field of ± 2 T collected at 1.8 K.

Table 1. Physical Properties of MPN 3 Assembled with PAMAM Dendrimers

sample	spacing (Å)	T_B (K)	H_C (Oe)	M_R/M_S (au)
Hex	64	83	500	0.30
G0.5	71	38	525	0.41
G1.5	74	33	525	0.42
G2.5	76	33	430	0.41
G3.5	79	32	540	0.41
G6.5	87	29	535	0.40
PS		29	525	0.40

increase in the blocking temperature even as we held the volume of the particles constant in each sample. A recent set of calculations by Kechrakos and Trohidou²¹ predict that the

(19) The nature of this discrepancy is unclear at this time; it is possible that the expected deviations are dampened by the low temperature.

(20) (a) Dormann, J. L.; Bessais, L.; Fiorani, D. *J. Phys. C* **1988**, *21*, 2015–2034. (b) Dormann, J. L.; Fiorani, D.; Tronc, E. *Adv. Chem. Phys.* **1997**, *98*, 283–494.

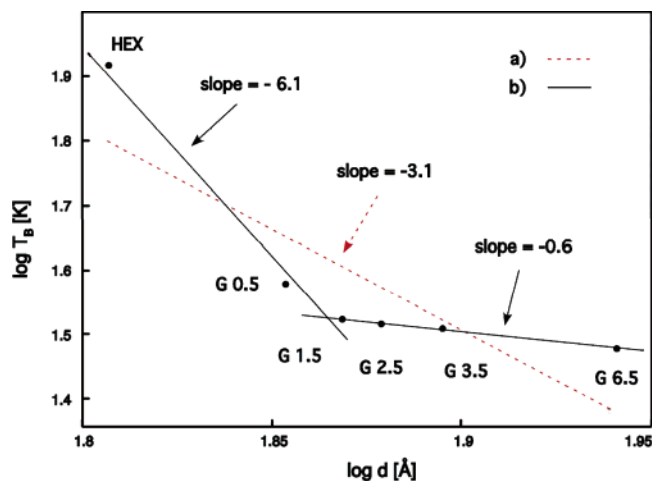


Figure 6. (a) Theoretical prediction of an inverse cubic relationship between T_B and interparticle spacing. (b) Experimental results indicating much stronger interactions at short range, rapidly reaching a plateau. (At relatively close interparticle spacings.)

blocking temperature of fine magnetic particles interacting through dipolar coupling should follow an inverse cubic dependence on interparticle spacing. To a first approximation our experimental data support this conclusion; however, there is systematic deviation. Closer analysis suggests an r^6 dependence on interparticle spacing up to an interparticle edge-to-edge spacing of just 1.0 nm, with a substantial leveling off above generation 1.5 (Figure 6). This trend suggests that past a certain interparticle spacing very little interaction penalty is present, allowing particles spaced beyond this threshold to act seemingly independent of one another. The ability to substantially reduce dipolar coupling between particles could have a significant impact on applications that require “independent” magnetic domains within a confined space. We are currently fabricating materials based upon other nanoparticle core materials to determine the generality of this behavior.

Finally we wanted to demonstrate the effectiveness of this method toward magnetically decoupling particles while retaining high particle density. To this end, we prepared a sample of particles under dilution conditions in an inert PS matrix. The blocking temperature of this sample should represent particles free of interparticle interactions (Figure 7). We found that the blocking temperature of this matrix-diluted sample was identical to that of the particles assembled with the largest dendrimer (generation 6.5), consistent with the presence of uncoupled particles within the dendrimer–particle nanocomposite.²²

This observation is in stark contrast to the earlier dilution studies where the statistical distribution, in terms of interparticle spacing, required to eliminate particle interactions is orders of magnitude larger than we report here. The key difference is our use of molecular self-assembly to specifically control the interparticle spacing of every nanoparticle in the sample, allowing us to take advantage of the dramatic dependence of collective behavior on interparticle spacing and create densely packed materials with negligible interparticle interactions.

In conclusion, we have shown that dendrimer-mediated assembly of magnetic particles directly modulates their collective behavior. This result can be explained in the context of an

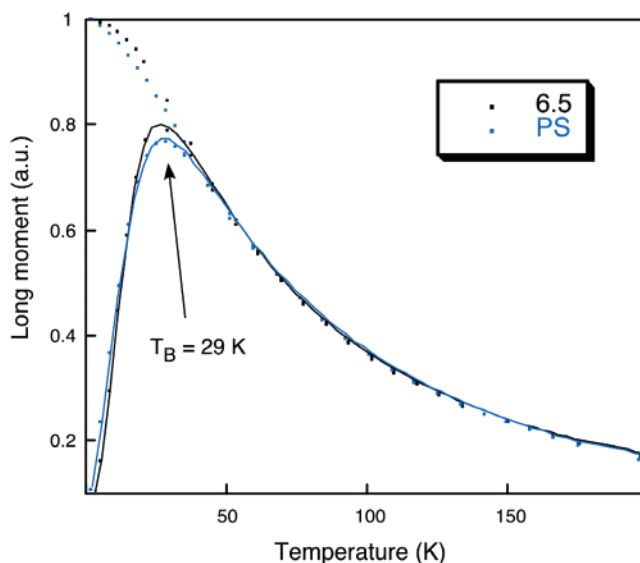


Figure 7. Zero-field-cooled and field-cooled experiments show identical behavior for the G6.5 assembled sample and a PS dilution.

increase in activation energy associated with an increase in interparticle dipolar coupling. The dependence of blocking temperature on interparticle spacing was found to deviate from a recent theoretical model and point toward a much more dramatic interdependence at close interparticle spacing, and a weaker correlation at larger spacings. As a result, we found that a relatively modest increase in interparticle spacing was enough to suggest fully independent particles within a dense assembly. We are currently undertaking a more rigorous set of experiments coupled to micromagnetic modeling to further understand this result.

Experimental Section

Nanoparticles MPN 1 and MPN 3 were prepared using the Alivisatos method¹³ and exchanged using 1,3-diol chemistry developed in our laboratory.²³ Briefly, particles were synthesized at high temperature from the decomplexation of iron cupferron and capped with a mixture of octylamine and triethylamine, resulting in a monolayer-protected nanocrystal (MPN 1) with a core diameter of 5.4 ± 1.2 nm.²⁴ Particles were then isolated by the addition of ethanol and redissolved in a 1:1 mixture of toluene and chloroform. A 1:1.5 ratio by weight of 1,3-diol ligand 2 to nanoparticle was added to an Ar-sparged solution and stirred at 50 °C for 2 days, during which time the particles precipitated, resulting in MPN 3 (Figure 1). The solvent was decanted, and the precipitate was washed repeatedly with chloroform to remove any free 1,3-diol ligand; the particles were then dissolved in methanol. A sample of particles from an identical batch was diluted into a sample of polystyrene at a weight ratio of 0.25% to approximate particles free from dipolar interactions. In addition, a sample of MPN 3 was prepared in the absence of dendrimer mortar, representing particles “fully” coupled, that is to say particles separated only by their respective monolayers.

Assembly. Dendrimer-mediated assembly followed from our earlier studies.^{11c} One milliliter samples of dendrimer, in methanol, were prepared at a concentration of 1.5×10^{-3} M. Fifty microliters of ~ 10 mg/mL solution of MPN 3 was briefly sonicated (less than 1 min to aid in dispersion) and added to the stock solution of dendrimer, at which time rapid precipitation took place. In the case of generations 3.5 and higher, gentle centrifugation was used to pellet the slowly assembling

(21) Kechrakos, D.; Trohidou, K. N. *Appl. Phys. Lett.* **2002**, *81*, 4574–4576.

(22) See Supporting Information for SAXS of PS-diluted sample.

(23) Boal, A. K.; Das, K.; Gray, M.; Rotello, V. M. *Chem. Mater.* **2002**, *14*, 2628–2636.

(24) See Supporting Information for TEM and histogram.

particles after 24 h. Assemblies were transferred to Kapton film, allowed to dry, and then analyzed using small-angle X-ray scattering (SAXS) and superconducting quantum interference device (SQUID) measurements. Identical samples were used for both the SQUID and SAXS analyses.

Characterization. (a) SAXS. Cu K α X-rays (1.54 Å) were generated in an Osmic MaxFlux source with a confocal multilayer optic (OSMIC, Inc.). Images were taken with a Molecular Metrology, Inc., camera consisting of a three-pinhole collimation system, 150 cm sample-to-detector distance (calibrated using silver behenate), and a two-dimensional, multiwire proportional detector (Molecular Metrology, Inc.). The entire X-ray path length was evacuated from the optic to the detector in order to reduce the background from air scattering. This setup allowed neglecting the correction for background scattering, as proved by experiment. Two-dimensional images were reduced to the one-dimensional form using angular integration. Scattering vectors (q) were calculated from the scattering angles (θ) using $q = 4\pi \sin \theta/\lambda$, and periodicities (D) were calculated from the principal scattering maxima (q^*) using $D = 2\pi/q^*$.

(b) SQUID. The samples used for SAXS were carefully transferred to the appropriate holder for analysis on an MPMS-7 SQUID magnetometer from Quantum Design. Zero-field-cooled and field-cooled (ZFC and FC) measurements were acquired with an applied field of 100 Oe between 1.8 and 300 K. Blocking temperature values were obtained

from fitting the curves to a canned Gaussian using IGOR. Hysteresis measurements ($\pm 20\,000$ Oe) were collected at 1.8 K and were mathematically subtracted to account for diamagnetic tilt and normalized to the saturation magnetization.

(c) IR. One to two milligrams of sample was incorporated into a KBr pellet and imaged on an MIDAC spectrophotometer, model number M1200-SP3.

(d) TEM. Transmission electron microscopy images were acquired using a JEOL 100CX instrument operating at an accelerating voltage of 100 keV. Each sample was prepared by drop-casting onto a carbon-coated copper grid and imaged after drying.

Acknowledgment. This research was supported by the National Science Foundation (CHE-0304173 and CHE-0213354). B.L.F. recognizes the ACS Division of Organic Chemistry and Proctor and Gamble for a graduate fellowship and the University of Massachusetts University Fellowship for support.

Supporting Information Available: Full synthetic details including TEM, IR, and additional SQUID analysis. This material is available free of charge via the Internet at <http://pubs.acs.org>.

JA051351M